Structure-Based Inhibitors of Influenza Virus Sialidase. A Benzoic Acid Lead with Novel Interaction†

Sangeeta Singh,‡ Marek J. Jedrzejas,§,⊥ Gillian M. Air,§ Ming Luo,§,⊥ W. Graeme Laver,|| and Wayne J. Brouillette*,‡

Departments of Chemistry and Microbiology and Center for Macromolecular Crystallography, University of Alabama at Birmingham, Birmingham, Alabama 35294, and John Curtin School of Medical Research, Australian National University, Canberra 2601, Australia

Received November 23, 1994®

Influenza virus sialidase is a surface enzyme that is essential for infection of the virus. The catalytic site is highly conserved among all known influenza variants, suggesting that this protein is a suitable target for drug intervention. The most potent known inhibitors are analogs of 2-deoxy-2,3-didehydro-*N*-acetylneuraminic acid (Neu5Ac2en), particularly the 4-guanidino derivative (4-guanidino-Neu5Ac2en). We utilized the benzene ring of 4-(*N*-acetylamino)benzoic acids as a cyclic template to substitute for the dihydropyran ring of Neu5Ac2en. In this study several 3-(*N*-acylamino) derivatives were prepared as potential replacements for the glycerol side chain of Neu5Ac2en, and some were found to interact with the same binding subsite of sialidase. Of greater significance was the observation that the 3-guanidinobenzoic acid derivative (equivalent to the 4-guanidino grouping of 4-guanidino–Neu5Ac2en), the most potent benzoic acid inhibitor of influenza sialidase thus far identified (IC_{50} = 10 μM), occupied the glycerol-binding subsite on sialidase as opposed to the guanidino-binding subsite. This benzoic acid derivative thus provides a new compound that interacts in a novel manner with the catalytic site of influenza sialidase.

Introduction

Influenza subtypes A and B both cause serious disease in man, each year resulting in excess morbidity and mortality, particularly in the elderly. Vaccines are in use but must be reformulated each year in response to antigenic variation and are frequently ineffective against new influenza variants. The only anti–influenza drugs currently licensed in the United States are amantadine and the structurally related rimantidine. These drugs act by blocking the viral-coded ion channel (M2 protein) in influenza A but are ineffective against influenza B, which uses a different ion channel. Also, resistance to these drugs typically develops quickly, limiting their usefulness. New, broad spectrum anti-influenza drugs that act by different mechanisms are needed.

Influenza viruses are enveloped RNA viruses which contain two major surface glycoproteins, hemagglutinin and sialidase (also called neuraminidase or acylneuraminyl hydrolase, EC 3.2.1.18), that are responsible for the antigenic properties of the virus. For influenza A, the World Health Organization has classified nine subtypes (N1–N9) of sialidase (only N1 and N2 have been found in humans), in contrast to only one subtype for influenza B sialidase. These proteins are essential for infection and offer potential targets for antiviral drug development. Hemagglutinin is responsible for viral attachment to host cells by binding to terminal sialic acid residues of surface glycoconjugates, and it is also involved in mediating membrane fusion. Sialidase catalyzes the hydrolysis of α-glycosidic bonds to the terminal sialic acid residues of surface glycoconjugates on hemagglutinin during virus budding and on the host cell virus receptor to assist virus release and prevent aggregation. This hydrolase activity is also believed to assist with virus mobility through the sialic acid-rich mucus of the respiratory tract.

Sialidase is a 240 kDa protein that accounts for 5–10% of the viral protein and appears in electron micrographs as mushroom-shaped heads on thin stalks which project from the surface of the virion membrane. These are composed of four coplanar, roughly spherical subunits and consist of an N-terminal membrane-anchored domain, a stalk, and a globular head. Each subunit of the head contains a catalytic site and is a glycosylated polypeptide of about 50 kDa containing six β-sheets arranged in a propeller-like formation. A calcium-binding site is located in each of the four subunits (outside the catalytic site), and an additional calcium-binding site is located centrally between the four subunits of the heads. Proteolytic cleavage of the stalks provides heads that have been crystallized and are antigenically and catalytically active (even in the crystalline state). (For a review of influenza virus sialidase, see ref 1.)

The product of the enzyme reaction, sialic acid (*N*-acetylneuraminic acid, Neu5Ac), is a modest inhibitor; in our *in vitro* inhibition assays, the IC_{50} is >10 mM (see Table 2). One of the most potent (until recently; see below) synthetic inhibitors for sialidase, commercially available 2-deoxy-2,3-didehydro-*N*-acetylneuraminic acid (Neu5Ac2en) (K_i = 4 and 20 μM for flu A and B, respectively),[2a] was obtained by the simple dehydration of Neu5Ac and was discovered over 25 years ago[3] (see Chart 1).

† The coordinates of the inhibitor–sialidase complexes have been deposited with Protein Data Bank, Chemistry Department, Brookhaven National Laboratories, Upton, Long Island, NY 11973; file names 1INF, 1ING, and 1INH.

‡ Department of Chemistry, University of Alabama at Birmingham.

§ Department of Microbiology, University of Alabama at Birmingham.

⊥ Center for Macromolecular Crystallography, University of Alabama at Birmingham.

|| Australian National University.

® Abstract published in *Advance ACS Abstracts,* June 15, 1995.

0022-2623/95/1838-3217$09.00/0

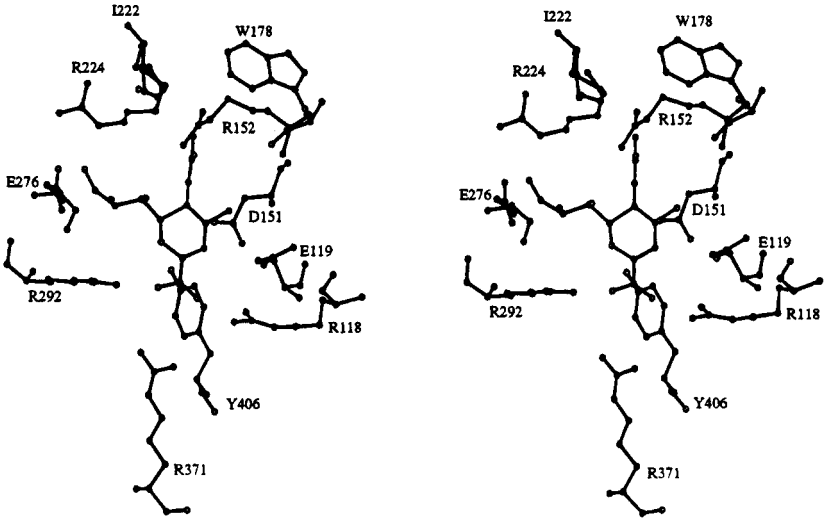

Figure 1. Structure of the catalytic site for the N2 sialidase–Neu5Ac2en complex. Shown are 11 completely conserved residues which directly contact Neu5Ac2en and compose four distinct binding subsites.

Chart 1

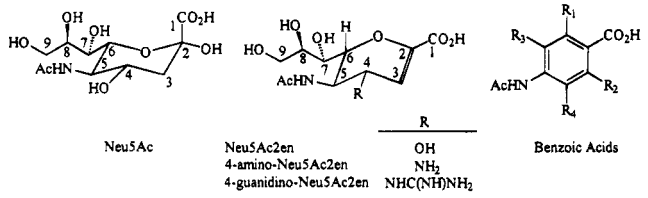

Several crystal structures of influenza sialidase and complexes with Neu5Ac and Neu5Ac2en have been reported.[4-11] While amino acid sequence identities among enzymes from different isolates may be less than 30%, the tertiary structures are highly conserved. Furthermore, the catalytic site of sialidase is completely conserved among all influenza A and B sources thus far investigated. The active site is a shallow crater formed primarily by charged amino acids via a first shell of 11 fully conserved residues, which directly contact Neu5Ac, and a second shell of mostly conserved residues which stabilize the binding site. Conservative site-directed mutations for these conserved residues usually result in inactivation,[1] suggesting that the virus may not easily evade sialidase-targeted drug therapy by mutation.

Recently, new synthetic analogs of Neu5Ac2en were prepared as potential sialidase inhibitors.[12,13] These efforts resulted in two new analogs with substitutions at C4: 4-amino-2,4-dideoxy-2,3-didehydro-*N*-acetylneuraminic acid (4-amino-Neu5Ac2en) and 4-guanidinino-2,4-dideoxy-2,3-didehydro-*N*-acetylneuraminic acid (4-guanidino-Neu5Ac2en) (see Chart 1). 4-Guanidino-Neu5Ac2en (K_i(app) = 10^{-9} M for N2) was more effective than 4-amino-Neu5Ac2en (K_i(app) = 10^{-8} M for N2) and inhibited a range of flu A and flu B neuraminidases.[2a] Furthermore, since 4-guanidino-Neu5Ac2en was observed to undergo slow binding, its steady state K_i may be even smaller.[14] Thus 4-guanidino-Neu5Ac2en is at least 1000 times more potent than Neu5Ac2en. Also, 4-guanidino-Neu5Ac2en is effective *in vivo* when given intranasally to both mice and ferrets,[12] but it is essentially inactive when administered by other routes (e.g., intraperitoneally)[2b] and rapidly excreted when administered iv (as similarly reported for Neu5Ac2en[15]). Several chicken viruses are not affected,[16] perhaps because they can spread without being released into nasal fluids.

Additionally, the relative chemical sensitivity (e.g., to acid, base, and heat) and the complex stereochemistry (five chiral centers) for this class of compounds appear to make the production of next generation agents problematic.

Our approach to the structure-based design of sialidase inhibitors uses the structure of the Neu5Ac2en–sialidase complex as a starting point and is based on the development of new classes of lead compounds by using chemically simpler cyclic templates in place of the dihydropyran ring of Neu5Ac2en. Our first choice for such an approach incorporated the benzene ring template, and we verified the validity of this approach by showing crystallographically that simple 4-(*N*-acetylamino)benzoic acids containing the equivalent of the C4-hydroxyl group on Neu5Ac2en were bound in the same orientation as Neu5Ac2en in the catalytic site of sialidase.[17] Furthermore, these preliminary compounds were modest *in vitro* inhibitors of influenza sialidase with potencies comparable to or better than that of sialic acid. Here we describe further studies of benzoic acid analogs of Neu5Ac2en containing side chains which substitute for the C6-glycerol grouping. We reveal that, in the crystalline sialidase complex, the structurally nonconstrained guanidinium group of 4-(*N*-acetylamino)-3-guanidinobenzoic acid (**113**) prefers to occupy the C6-glycerol-binding subsite of Neu5Ac2en rather than, as observed with 4-guanidino-Neu5Ac2en, the C4-hydroxyl-binding subsite.

Design

The Neu5Ac2en–sialidase crystal structure was used as a starting point. The very tight interaction of this ligand's carboxylate with three arginine residues (N2 numbering: Arg 118, 292, and 371) and the interactions of the *N*-acetyl methyl group with the only hydrophobic region in the catalytic site of sialidase (Ile 222 and Trp 178) and of the amide carbonyl oxygen with Arg 152 suggested that these groupings are likely important for orientation in the binding site. It appeared that these two groupings should therefore be incorporated, with the proper orientation and spacing, in all new structures. This should be possible using cyclic templates other than the dihydropyran ring of Neu5Ac2en that, in addition, structurally provide opportunities for ex-

Table 1. Structures for the Benzoic Acid Analogs That Were Evaluated in This Study

compd	R_1	R_2	R_3	R_4
101	H	H	H	OH
102	H	H	H	OAc
103	NO_2	NO_2	H	OH
104	H	H	NO_2	OAc
105	H	H	NO_2	OH
106	H	H	NH_2	OH
107	H	H	H	NO_2
108	H	H	H	NH_2
109	H	H	H	$NHCOCH_2OH$
110	H	H	H	$NHCOCH(OH)CH_2OH$
111	H	H	H	$NHCOCH_2NH_2$
112	H	H	H	$NHCO(CH_2)_3NH_2$
113	H	H	H	$NHC(NH)NH_2$

ploring all binding subsites utilized by Neu5Ac2en as well as new binding subsites. The benzene ring was selected as the first template because it accomplishes the above goals and, in addition, provides planarity near the carboxylate believed to be important for assuming the transition-state-like structure of Neu5Ac2en and its derivatives.[6,18] Also, the benzene ring is relatively rigid and thus simplifies the prediction of favorable side chain presentation to the catalytic site, contains comparatively simple stereochemistry (no chiral centers are present at ring to side chain junctions), and in general provides for straightforward synthetic procedures. The suitability of newly proposed structures for the exploration of binding subsites occupied by Neu5Ac2en was first evaluated using molecular modeling by fitting energy-minimized benzoic acid targets [using Maximin 2 within Sybyl 6.0 (Tripos Assoc.)] with the structure of Neu5Ac2en as it is bound in the sialidase active site. Potential compounds were also investigated qualitatively in the sialidase binding site for reasonable steric and electrostatic complementarity using FRODO.[19] These considerations led to the preparation and evaluation of the preliminary benzoic acid series whose structures are summarized in Table 1. The relative ordering of inhibitor potency has been correctly calculated[20] for several of the benzoic acids using DelPhi,[21] and these calculations are being employed to further assist with future inhibitor design. Finally, the program GRID[22] has been employed to help evaluate the possibility of using alternate functionality to interact with the binding subsites occupied by Neu5Ac2en and to identify new functionality for additional binding subsites in the sialidase catalytic site that are not occupied by the functionality of Neu5Ac2en.

Chemistry

Benzoic acids **102** and **104**–**108** were synthesized from 4-(*N*-acetylamino)benzoic acid or 4-amino-3-hydroxybenzoic acid.[17] The syntheses of **101** and **103** are summarized in Scheme 1. In this procedure **102** underwent selective hydrolysis of the acetate ester under basic conditions to provide a 50% yield of **101**. An early attempt to mononitrate **102** in HNO_3 and H_2SO_4 resulted in cleavage of the acetate ester to give dinitro product **103** in 67% yield. Thus milder nitrating conditions were subsequently utilized for this and other acetoxybenzoic acids.

The synthesis of **113** was accomplished in 60% yield by heating **108** with cyanamide in aqueous HCl as summarized in Scheme 2. Also shown in Scheme 2 are

Scheme 1

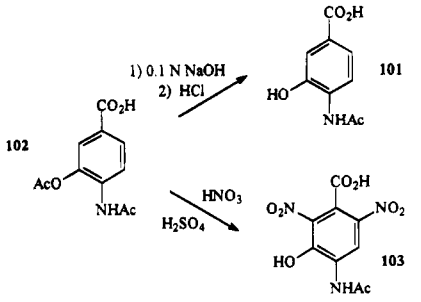

Scheme 2

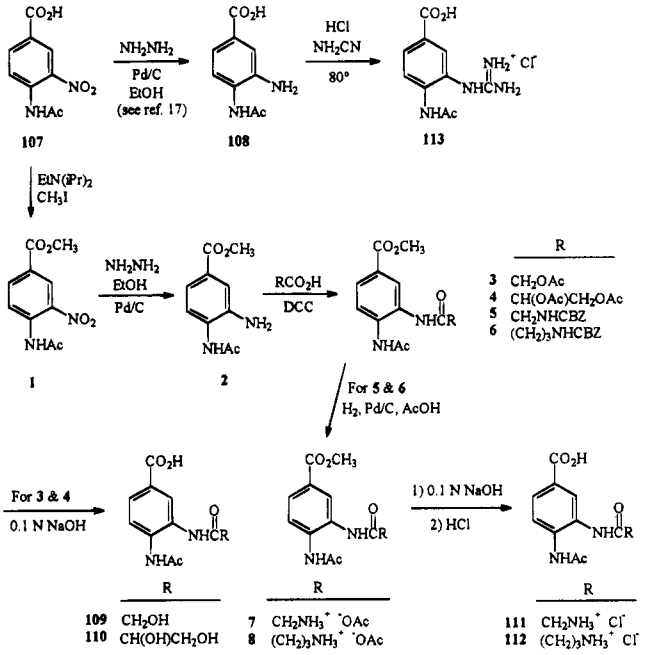

the preparations of **109**–**112**. The general approach involved protection of the carboxylic acid in **107** via treatment with methyl iodide under basic conditions to give ester **1** in 94% yield. The nitro group in **1** was reduced using transfer hydrogenation to provide amine **2** in 79% yield, and **2** was then reacted with a variety of N- or O-protected amino- or hydroxy-substituted carboxylic acids in the presence of DCC to yield intermediate amides **3**–**6** in good yield. The O-protecting groups of **3** and **4**, along with the methyl ester, were hydrolyzed using aqueous base to provide **109** and **110** in 58% and 97% yields, respectively. The N-protecting groups of **5** and **6** were removed using hydrogenolysis to provide amines **7** and **8** in 66% and 83% yields, respectively, and the methyl esters underwent base-catalyzed hydrolysis to give **111** and **112** in respective yields of 84% and 81%.

Biological Assays

All compounds were evaluated for *in vitro* inhibitory actions on influenza N2 (A/Tokyo/67) and influenza type B (B/Memphis/3/89) sialidases in whole virus using two different substrates according to a published method.[23] The IC_{50} values were determined graphically and are summarized in Table 2.

Due to the greater potency of **113** in the above assays, it was further evaluated for effects on virus production in a preliminary screen. The continuous cultured cells used for growing influenza A and B viruses were

Table 2. *In Vitro* Inhibitory Effects of Benzoic Acid Analogs on Influenza A and B Sialidases in Whole Virus (IC_{50}, mM)

	MUN		fetuin	
compd	N2	B/Mem/89	N2	B/Mem/89
101	>10	>10	10	10
102	>10	>10	10	5
103	1	1	3	4
104	5	2	3	5
105[a]	0.75	0.75	1	1
106[a]	>10	10	>10	>10
107	5	5	5	5
108[a]	>10	>20	>10	N/D[b]
109	4	3	>10	10
110	5	8	4	>10
111	5	5	5	5
112	>10	>10	>10	>10
113	0.01	0.01	0.01	0.01
Neu5Ac	N/D	>10	N/D	N/D
Neu5Ac2en	0.015	0.015	0.015	0.015

[a] Data taken from ref 17. [b] N/D: not determined.

Table 3. Summary of Refinement Results for Sialidase–Benzoic Acid Complexes

						rms	
complex	no. of reflectns	R_{sym} (%)	R_{es} (Å)	R (%)	no. of H_2O	bond (Å)	angle (deg)
N2–**109**	21 389	11.7	1.9	18.2	0	0.012	1.955
N2–**111**	21 819	10.6	1.9	16.5	125	0.012	2.016
B/Lee–**113**	19 538	10.0	1.9	16.3	125	0.012	2.156

Madin–Darby canine kidney (MDCK) cells. When the MDCK cells became confluent, they were inoculated with influenza virus A/Tokyo/67 and **113** was then added at several concentrations (10-fold dilutions) that spanned the IC_{50} value. At 48 h postinfection the supernatant from the infected cells was harvested and the viral yield was determined from the HA titer. Under these conditions, the IC_{50} value for **113** was estimated as 1–10 μM.

X-ray Crystal Structures of Benzoic Acid–Sialidase Complexes

Crystals of native N2 neuraminidase (A/Tokyo/3/67) were grown by the hanging drop method using purified sialidase heads, and the crystallization of B/Lee/40 was accomplished according to a published procedure.[24] The benzoic acid–sialidase complexes were prepared by placing the native N2 or B/Lee/40 crystals in an aqueous soaking buffer (containing 5% DMSO) containing inhibitors (5 mM) for about 8 h. The diffraction data were collected at room temperature on a SIEMENS multiple wire area detector using Cu Kα radiation. The data were processed using the XENGEN package, the inhibitors were incorporated after initial rigid body refinements of the protein, and the complexes were then refined using the X-plor protocol. The final results of refinement for the complexes are given in Table 3.

Results and Discussion

As demonstrated by several published crystal structures for the Neu5Ac2en–sialidase complex, each of the side chains on Neu5Ac2en interacts with conserved amino acid residues in the sialidase catalytic site. The interactions observed for the carboxylate and *N*-acetyl subsites were discussed above. Additionally, the C4-hydroxyl group on Neu5Ac2en occupies a subsite near Asp 151 and Glu 119. For the C6-glycerol side chain, only the C8- and C9-hydroxyls undergo interactions with the binding site via Glu 276.

Employing the benzene template, we have first explored the ability of benzoic acid derivatives to provide side chains capable of interacting with the binding subsites occupied by Neu5Ac2en. Table 1 summarizes the structures that were evaluated. We previously determined the benzoic acid–sialidase complex crystal structures for benzoic acid derivatives which contain a *m*-hydroxyl group (the equivalent of the C4-hydroxyl group on Neu5Ac2en), amino group, and/or nitro group (**105**, **106**, and **108**).[17] While these compounds were only modest *in vitro* inhibitors of sialidase, our studies revealed that benzoic acid derivatives bind in the sialidase catalytic site, orient the benzene ring like the dihydropyran ring of Neu5Ac2en, and place the carboxylate and *N*-acetylamino groups in the same binding subsites. Furthermore, the *m*-hydroxyl grouping in benzoic acid derivatives occupies the C4-hydroxyl-binding subsite of Neu5Ac2en, suggesting the suitability of this class of compounds for further elaboration.

In the present study we have evaluated alternate meta substituents in the benzoic acid series which should be capable of undergoing interactions resembling those for the C6-glycerol side chain of Neu5Ac2en. For reasons of ready synthetic accessibility, we utilized the hydroxyl- and amino-substituted acylamino groupings contained in **109**–**112**. In Neu5Ac2en only the C8- and C9-hydroxyl groups interact with the catalytic site; compound **109** contains the same size side chain as the glycerol group in Neu5Ac2en (i.e., three linking atoms between the ring and the terminal hydroxyl group) and a terminal hydroxyl that is equivalent to the C9-hydroxyl of Neu5Ac2en. The side chain in **111** is the same size but terminates in a charged primary ammonium group, which might form a more favorable salt bridge interaction with Glu 276 as compared to a hydroxyl group (such a salt bridge interaction to Glu 119 was used to rationalize the enhanced binding activity of 4-amino-Neu5Ac2en over Neu5Ac2en).[12] Compound **110** contains two hydroxyl groupings which provide functionality approximating that of both the C8- and C9-hydroxyls of Neu5Ac2en. However, in this case the side chain contains four linking atoms, as opposed to three linking atoms for Neu5Ac2en, and it was anticipated that tilting of the benzene ring in the catalytic site would be required for the proper interactions of this compound with Glu 276.

Once their syntheses were completed, **109**–**111** were evaluated *in vitro* with whole virus for their ability to inhibit influenza sialidase. The results of these studies are summarized in Table 2. As shown, all were of comparable activity and only slightly more potent than sialic acid (Neu5Ac).

Two of these compounds, **109** and **111**, were soaked into N2 crystals, and the structures for the sialidase complexes were determined. The complex structures are shown in Figure 2. For these compounds the terminal OH or NH_3^+ groupings hydrogen bond to Glu 276. The distance between the carboxylate oxygen on Glu 276 and the terminal O or N of **109** or **111** is less than 3.0 Å, which is within normal hydrogen-bonding distance. A comparison of the sialidase inhibition data in Table 2 for **101**, **106**, **109**, and **111** suggests that the single hydrogen-bonding interaction provided by the

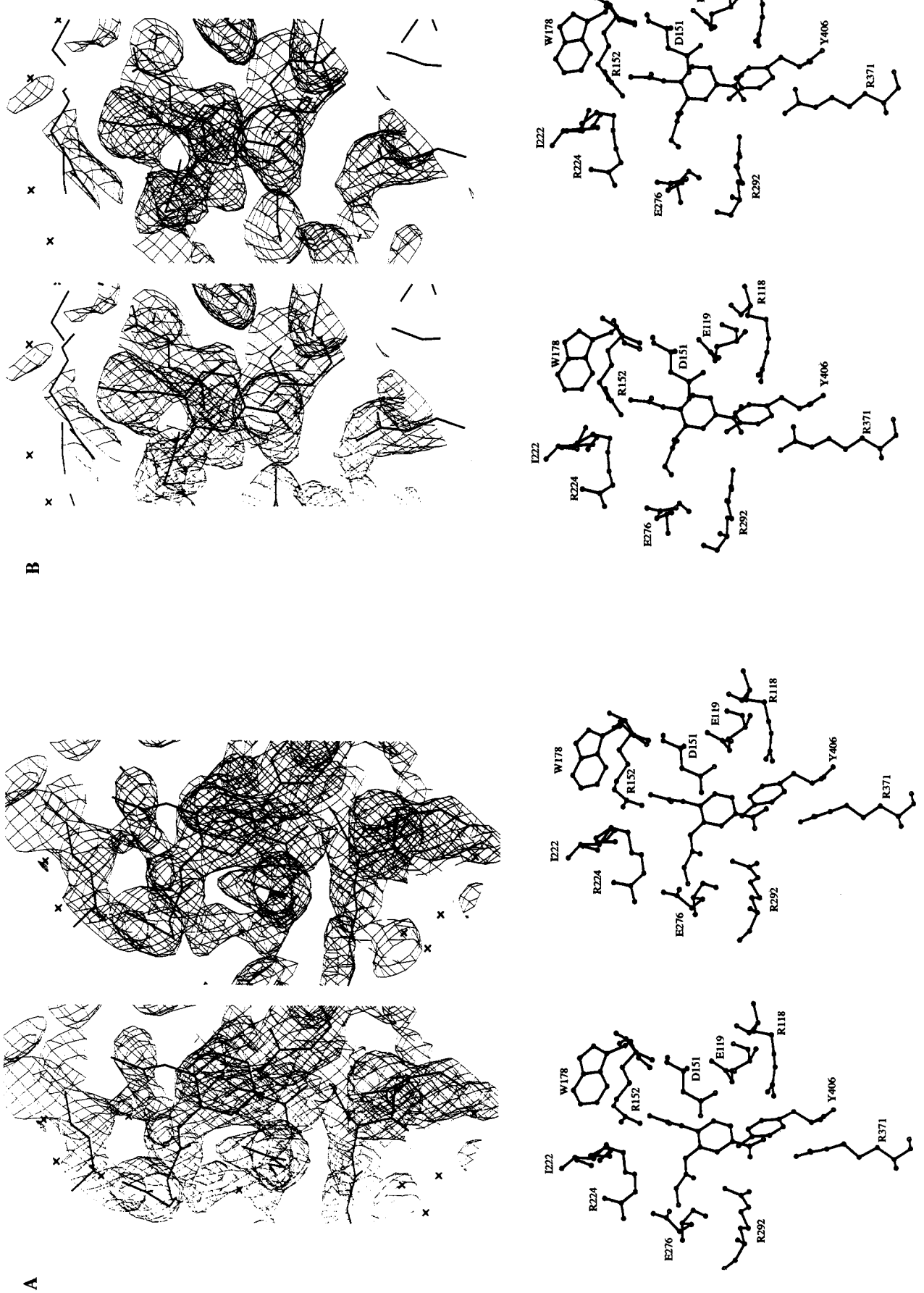

Figure 2. Electron density maps and structures for (A) the N2–**109** complex and (B) the N2–**111** complex. Both ligands orient like Neu5Ac2en in the binding site, and the side chain of each occupies the glycerol-binding subsite via interaction with E276.

side chain of the latter two compounds is roughly as effective as a *m*-OH group, which interacts with Asp 151 on the opposite side of the benzene ring, for enhancement of binding. The implication is that multiple interactions of this type may significantly improve binding.

As described earlier, the most potent inhibitor of sialidase thus far described is an analog of Neu5Ac2en containing a guanidinium group at C4 in place of the 4-hydroxyl group. The 4-guanidino-Neu5Ac2en–sialidase complex structure has been described,[12] revealing that this inhibitor orients in the sialidase catalytic site like Neu5Ac2en, maintaining the same subsite interactions for the carboxylate, *N*-acetyl, and glycerol groupings. However, the guanidino grouping undergoes lateral bonding between Glu 227 and 119. The extra interaction with Glu 227 (as compared to Neu5Ac2en, which does not interact with Glu 227) was initially suggested as the reason for the dramatically enhanced binding affinity of 4-guanidino-Neu5Ac2en,[12] although a later report[25] also suggested contributions to the high binding affinity from (a) entropy gains resulting from the expulsion of an ordered water molecule located in this binding subsite and (b) favorable van der Waals forces between the bulky guanidinium group and adjacent enzyme active-site residues.

In order to determine the effect of a guanidino group on binding activity within the benzoic acid series, compound **113** was synthesized. As shown in Table 2 this compound was about 100 times more effective than any of the previous benzoic acid analogs as a sialidase inhibitor.

Compound **113** was soaked into a crystal of B/Lee/40 sialidase, and the complex structure was determined (Figure 3). It was anticipated that the guanidino group of **113** would occupy the same binding subsite observed with the 4-guanidino-Neu5Ac2en–sialidase complex. However, in this case the guanidino group occupied the *glycerol*-binding subsite of Neu5Ac2en, forming a salt bridge interaction with Glu 275. The C–C distance between **113**'s guanidino group and the carboxylate of Glu 275 is roughly 4.2 Å, which is about the same distance observed for the similar interaction between the carboxylate of Neu5Ac2en and the guanidinium group of Arg 371.

Unlike the dihydropyran ring of Neu5Ac2en and its analogs, the 4-(*N*-acetylamino)benzoic acid ring is symmetrical. Since there are no structural constraints, the guanidinium group of **113** has equivalent opportunities to bind in 4-guanidino-Neu5Ac2en's guanidinium subsite or glycerol subsite, requiring only a 180° rotation of the benzene ring. This result, in fact, reveals that a single guanidinium grouping, at least when attached to a benzoic acid ring, undergoes more energetically favorable interactions with 4-guanidino-Neu5Ac2en's glycerol-binding subsite on sialidase as compared to the guanidinium-binding subsite.

These studies thus provide a new structural class of sialidase inhibitors and describe one example that interacts in a unique manner with the catalytic site.

Experimental Section

Chemistry. General Procedures. Melting points were obtained on an Electrothermal melting point apparatus and are uncorrected. ^{1}H NMR spectra were recorded on Varian EM 360 (60 MHz) and GE 300-WB FT-NMR (300 MHz) spectrometers. IR spectra were recorded on a Perkin Elmer 1310 infrared spectrophotometer. GC/MS data were recorded on a Hewlett-Packard 5985 spectrometer. TLC was performed on Sigma brand silica gel GF plates (0.2 mm layer). Elemental analyses were provided by Atlantic Microlabs of Atlanta, Georgia.

Compounds **102** and **104–108** were prepared from 4-(*N*-acetylamino)benzoic acid or 4-amino-3-hydroxybenzoic acid.[17]

4-(Acetylamino)-3-hydroxybenzoic Acid (101). A solution of **102** (100 mg, 0.42 mmol) in 0.1 N NaOH (5 mL) was stirred at room temperature for 30 min. Concentrated HCl was added dropwise to adjust the mixture to pH 2, and this was extracted with ethyl acetate (2 × 10 mL). The extracts were dried (Na_2SO_4) and concentrated to dryness on a rotary evaporator, and the solid residue was washed out of the flask with hexane and filtered to give **101** (40 mg, 49% yield): mp 249–250 °C (lit.[26] mp 245–248 °C).

4-(Acetylamino)-3-hydroxy-2,6-dinitrobenzoic Acid (103). Compound **102** (2.00 g, 8.43 mmol) was added gradually to a paste made from concentrated H_2SO_4 (8.5 mL) and potassium nitrate (2.22 g, 22.0 mmol) at −10–0 °C. The reaction mixture was stirred at 0 °C for 1 h, and the syrupy mass was poured onto cracked ice. After standing for 20 min, a yellow solid separated. This was filtered, washed on the filter with cold water, and air-dried to give **103** (1.60 g, 66.7% yield): mp 200–203 °C (ethyl acetate/hexane); IR (KBr) 3400, 2700–2500, 1720, 1650 cm^{-1}; MS *m/z* 285 (M$^+$); ^{1}H NMR (300 MHz, DMSO-d_6) δ 2.16 (s, 3 H, $NCOCH_3$), 8.73 (s, 1 H, aromatic), 9.72 (s, 1 H, NH); ^{13}C NMR (75.5 MHz, DMSO-d_6) δ 172.30, 165.20, 148.02, 143.20, 141.23, 140.00, 123.20, 120.05, 23.30. Anal. ($C_9H_7N_3O_8$) C, H, N.

Methyl 4-(Acetylamino)-3-nitrobenzoate (1). Compound **107** (1.50 g, 6.69 mmol) was dissolved in DMF (25 mL), and diisopropylethylamine (16.0 g, 92.7 mmol) and MeI (2.3 mL, 5.2 g, 39 mmol) were added. This solution was stirred at room temperature for 24 h. The solid which formed was filtered, and the filtrate was concentrated to dryness on a rotary evaporator. The residue was dissolved in $CHCl_3$ (100 mL), washed with water (3 × 50 mL), dried (Na_2SO_4), and concentrated to provide **1** (1.50 g, 94.3%) as a yellow solid: mp 123–124 °C (ethanol) (lit.[27] mp 127 °C).

Methyl 4-(Acetylamino)-3-aminobenzoate (2). To a suspension of **1** (0.870 g, 3.65 mmol) in ethanol (30 mL) was added 10% Pd–C (0.87 g) and 5% HCl (0.85 mL). Hydrazine hydrate (55%, 0.850 mL, 0.470 g, 15.0 mmol) dissolved in ethanol (5 mL) was then added dropwise to the above mixture. The reaction mixture was stirred at room temperature for 1 h, and the Pd–C was filtered. The filtrate was concentrated under vacuum to give **2** (0.500 g, 78.7% yield) as a white solid: mp 187–190 °C (ethanol/ether); IR (KBr) 3400–3300, 1710, 1650, 1600 cm^{-1}; MS *m/z* 208 (M$^+$); ^{1}H NMR (300 MHz, DMSO-d_6) δ 2.06 (s, 3 H, $NCOCH_3$), 3.79 (s, 3 H, CO_2CH_3), 5.04–5.27 (br s, 2 H, NH_2), 7.11–7.18 (m, 1 H, aromatic), 7.34–7.39 (m, 1 H, aromatic), 7.44–7.53 (m, 1 H, aromatic), 9.10–9.18 (br s, 1 H, NH); ^{13}C NMR (75.5 MHz, DMSO-d_6) δ 168.41, 166.24, 140.65, 127.97, 125.89, 123.62, 117.10, 116.15, 51.67, 23.53. Anal. ($C_{10}H_{12}N_2O_3$) C, H, N.

Methyl 4-(Acetylamino)-3-[(acetoxyacetyl)amino]benzoate (3). Compound **2** (0.200 g, 0.960 mmol) was dissolved in a mixture of anhydrous DMF (2 mL) and anhydrous dioxane (5 mL), and the solution was cooled to 0–5 °C in an ice bath. To this were added acetoxyacetic acid (0.124 g, 0.129 mmol) and DCC (0.198 g, 0.210 mL, 0.960 mmol). The reaction mixture was stirred for a few minutes at 0 °C, the ice bath was removed, and the mixture was stirred at room temperature for 4 h. The solid which separated was filtered, and the filtrate was concentrated to dryness on a rotary evaporator. The solid residue was triturated with 5% HCl, filtered, and washed on the filter with water. The collected solid was then triturated with 5% $NaHCO_3$, filtered, washed with water, and dried under vacuum to give **3** (270 mg, 70.9% yield) as a white solid: mp 182–186 °C (ethyl acetate/hexane); IR (KBr) 3400–3100, 1740, 1720, 1660, 1640 cm^{-1}; MS *m/z* 308 (M$^+$); ^{1}H NMR (300 MHz, DMSO-d_6) δ 2.08 (s, 3 H, $NCOCH_3$), 2.18 (s, 3 H, $COCH_3$), 3.83 (s, 3 H, CO_2CH_3), 4.68 (s, 2 H, CH_2), 7.73–7.81 (m, 2 H, aromatic), 8.10–8.20 (m, 1 H, aromatic), 9.57 (br s, 1

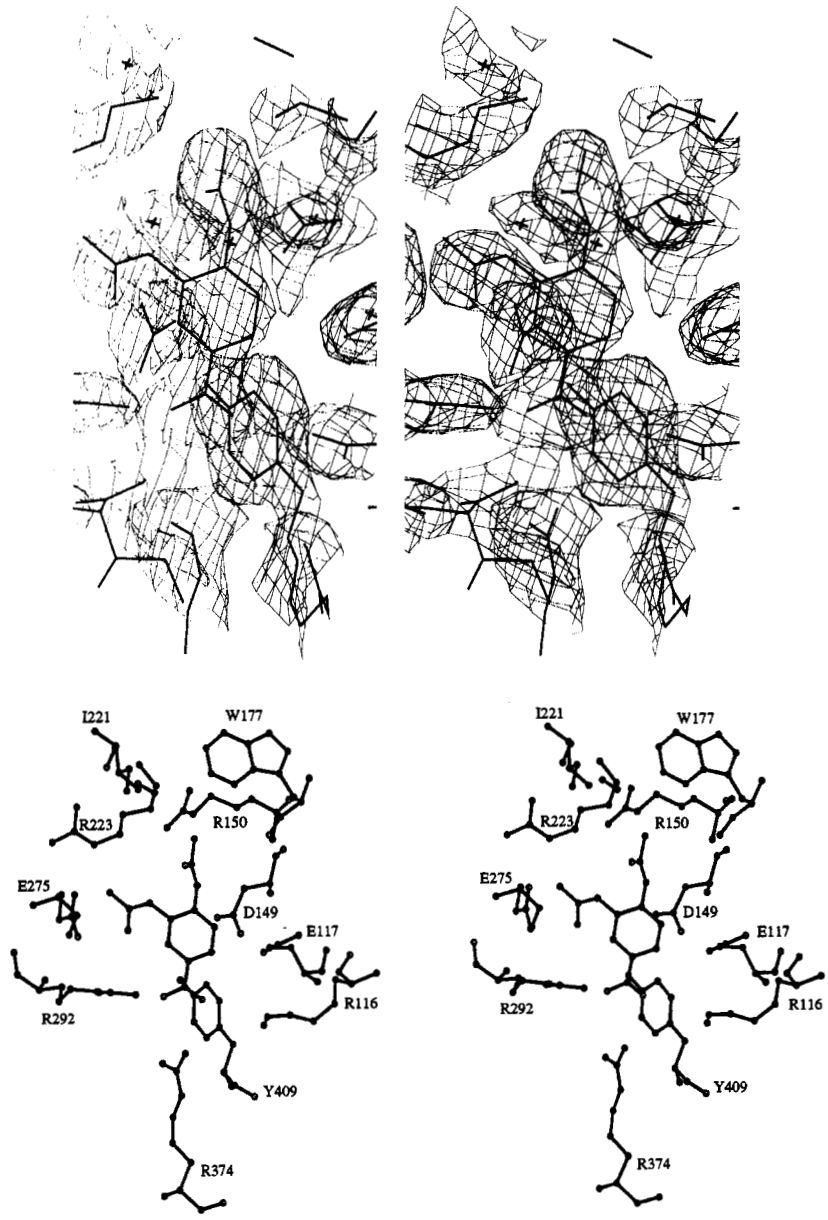

Figure 3. Electron density map and structure for the B/Lee−**113** complex. Unlike the guanidino group of 4-guanidino-Neu5Ac2en, which occupies the 4-hydroxy-binding subsite of Neu5Ac2en, the guanidino group of **113** occupies the glycerol-binding subsite in B/Lee sialidase.

H, NH), 9.65 (br s, 1 H, NH); ^{13}C NMR (DMSO-d_6) δ 170.85, 170.63, 167.27, 165.49, 136.85, 135.52, 128.95, 126.14, 124.25, 120.25, 63.40, 53.43, 23.65, 20.26. Anal. ($C_{14}H_{16}N_2O_6$) C, H, N.

Methyl 4-(Acetylamino)-3-[(2,3-diacetoxypropanoyl)-amino]benzoate (4). Compound **2** (0.12 g, 0.57 mmol) was reacted as described for the preparation of **3** using 2,3-diacetoxypropionic acid (0.220 g, 1.15 mmol) and DCC (0.195 mL, 0.183 g, 0.870 mmol) to afford **4** (200 mg, 91%) as a white solid: mp 132−134 °C (ethyl acetate/hexane); IR (mineral oil) 3400−3200, 1730, 1700, 1650, 1600 cm^{-1}; MS *m/z* 380 (M^+); ^{1}H NMR (300 MHz, DMSO-d_6) δ 2.10 (s, 3 H, $NCOCH_3$), 2.20 (s, 3 H, $OCOCH_3$), 2.28 (s, 3 H, $OCOCH_3$), 3.91 (s, 3 H, CO_2CH_3), 4.46−4.68 (m, 2 H, CH_2OCOCH_3), 5.43−5.49 (m, 1 H, $CHOCOCH_3$), 7.48−7.56 (m, 1 H, aromatic), 7.84−7.92 (m, 1 H, aromatic), 8.01−8.07 (br s, 1 H, NH), 8.07−8.11 (m, 1 H, aromatic), 8.74−8.84 (br s, 1 H, NH); ^{13}C NMR (DMSO-d_6) δ 169.09, 168.96, 166.27, 165.49, 136.82, 135.45, 128.93, 126.21, 125.19, 123.30, 72.76, 53.95, 23.89, 20.58, 20.50. Anal. ($C_{17}H_{20}N_2O_8$) C, H, N.

Methyl 4-(Acetylamino)-3-[[*N*-(benzyloxycarbonyl)-amino]acetyl]benzoate (5). Compound **2** (0.20 g, 0.96 mmol) was reacted with *N*-(benzyloxycarbonyl)glycine (0.320 g, 1.53 mmol) and DCC (0.295 g, 0.314 mL, 1.43 mmol), as described for the preparation of **3**, to give **5** (260 mg, 68% yield) as a white solid: mp 150−153 °C (ethyl acetate/hexane); IR (mineral oil) 3400−3100, 1720, 1650, 1590 cm^{-1}; MS *m/z* 399 (M^+); ^{1}H NMR (300 MHz, DMSO-d_6) δ 2.11 (s, 3 H, $NCOCH_3$), 3.79−3.95 (s, 5 H, CH_2NH, CH_3COO), 7.28−7.45 (m, 5 H, aromatic), 7.58−7.67 (br s, 1 H, NH), 7.67−7.87 (m, 2 H, aromatic), 8.06−8.20 (m, 1 H, aromatic), 9.41−9.54 (m, 2 H, NH); ^{13}C NMR (DMSO-d_6) δ 169.07, 168.54, 156.57, 136.82, 135.46, 128.90, 128.27, 126.12, 125.15, 123.25, 65.61, 52.02, 44.24, 23.68. Anal. ($C_{20}H_{21}N_3O_6$) C, H, N.

Methyl 4-(Acetylamino)-3-[[4-[*N*-(benzyloxycarbonyl)-amino]butanoyl]amino]benzoate (6). Compound **2** (200 mg, 0.960 mmol) was treated as described for the preparation of **3** with 4-[*N*-(benzyloxycarbonyl)amino]butyric acid (395 mg, 1.78 mmol) and DCC (0.32 mL, 0.300 g, 1.45 mmol) to give 570 mg of a crude solid, mp 125−167 °C. This was triturated with $CHCl_3$ (5 mL) and filtered to give **6** (200 mg, 60.0% yield) as a white solid: mp 168−171 °C (ethyl acetate/hexane); IR (mineral oil) 3300, 1710, 1680, 1650, 1600 cm^{-1}; MS *m/z* 427 (M^+); ^{1}H NMR (300 MHz, DMSO-d_6) δ 1.69−1.83 (m, 2 H, $CH_2CH_2CH_2$), 2.09 (s, 3 H, $NHCOCH_3$), 2.45−2.33 (m, 2 H, $CO\text{-}CH_2$), 3.04−3.11 (m, 2 H, NCH_2), 3.82 (s, 3 H, $COOCH_3$), 5.02 (s, 2 H, CH_2Ph), 7.32 (s, 5 H, aromatic), 7.65−7.67 (m, 1 H, aromatic), 7.80−7.87 (m, 1 H, aromatic), 8.10−8.14 (m, 1

H, aromatic), 9.32–9.46 (br s, 2 H, NH); ^{13}C NMR (DMSO-d_6) δ 171.33, 168.79, 165.54, 156.08, 137.10, 135.23, 129.20, 126.09, 125.90, 124.84, 123.35, 65.09, 51.94, 3.07, 25.25, 23.81. Anal. ($C_{22}H_{25}N_3O_6$) C, H, N.

Methyl 4-(Acetylamino)-3-[(aminoacetyl)amino]benzoate, Hydroacetate (7) and Methyl 4-(Acetylamino)-3-[(4-aminobutanoyl)amino]benzoate (8). A mixture of 10% Pd–C (80 mg), water (1 mL), and glacial acetic acid (1 mL) was stirred at room temperature under 1.0 atm of hydrogen gas for 1 h. A solution of **5** (150 mg, 0.375 mmol) or **6** (100 mg, 0.234 mmol) in glacial acetic acid (5 mL) was then added, and the reaction mixture was stirred at room temperature for 24 h. The catalyst was removed by filtration and washed on the filter with water (5 mL), and the filtrate was concentrated to dryness on a rotary evaporator to give an oily residue. This was dissolved in water (10 mL) and extracted once with ethyl acetate (10 mL), and the aqueous layer was concentrated to dryness on a rotary evaporator. The oily residue was dried under vacuum to give **7** (80 mg, 66% yield) as an oil or **8** (70 mg, 83%) as a solid.

7: IR (mineral oil) 3400–3100, 1720, 1640 cm^{-1}; ^{1}H NMR (300 MHz, DMSO-d_6) δ 1.89 (s, 3 H, $CH_3CO_2^-$), 2.10 (s, 3 H, $NCOCH_3$), 3.33 (s, 2 H, CH_2N), 3.84 (s, 3 H, CH_3OCO), 7.61–7.81 (m, 2 H, aromatic), 8.38–8.47 (m, 1 H, aromatic), 9.78–9.97 (br s, 1 H, NH); ^{13}C NMR (D_2O) δ 169.46, 168.67, 156.75, 136.7, 135.56, 129.01, 125.90, 125.25, 123.45, 52.14, 44.42, 23.59. Anal. ($C_{14}H_{19}N_3O_6$) C, H, N.

8: mp 200–204 °C; IR (mineral oil) 3450–3200, 1700, 1650, 1590 cm^{-1}; ^{1}H NMR (300 MHz, DMSO-d_6) δ 1.87–1.94 (m, 5 H, $CH_2CH_2CH_2$, $CH_3CO_2^-$), 2.14 (s, 3 H, $NCOCH_3$), 2.51–2.60 (m, 2 H, CH_2CO), 2.80–2.94 (m, 2 H, NCH_2), 3.81–3.84 (s, 3 H, $COOCH_3$), 7.67–7.64 (m, 1 H, aromatic), 7.84–7.94 (m, 4 H, aromatic, NH_3^+), 8.18–8.22 (m, 1 H, aromatic), 9.84–9.89 (br s, 2 H, NH); ^{13}C NMR (D_2O) δ 170.23, 169.16, 165.42, 137.20, 135.42, 129.32, 125.80, 124.95, 123.40, 51.94, 33.07, 40.04, 25.31, 23.81. Anal. ($C_{16}H_{23}N_3O_6$) C, H, N.

4-(Acetylamino)-3-[(hydroxyacetyl)amino]benzoic Acid (109) and 4-(Acetylamino)-3-[(2,3-dihydroxypropanoyl)-amino]benzoic Acid (110). Compound **3** (0.200 g, 0.652 mmol) or **4** (0.140 g, 0.368 mmol) was dissolved in 0.1 N NaOH (8 mL) and stirred at room temperature for 2 h (for **3**) or at 0 °C for 1 h (for **4**). The alkaline aqueous layer was acidified to pH 2–3 with concentrated HCl and extracted with ethyl acetate (2 × 15 mL), and the extracts were dried (Na_2SO_4) and concentrated on a rotary evaporator to give **109** (60 mg, 58% yield) or **110** (100 mg, 97.0% yield) as white solids.

109: mp 214–215 °C (ethanol); IR (mineral oil) 3400–2700, 1690, 1650, 1600 cm^{-1}; ^{1}H NMR (300 MHz, DMSO-d_6) δ 2.09 (s, 3 H, $NCOCH_3$), 4.00 (s, 2 H, CH_2OH), 5.69 (br s, 1 H, OH), 7.47–7.55 (m, 1 H, aromatic), 7.59–7.75 (m, 1 H, aromatic), 9.35 (s, 1 H, NH), 9.75 (s, 1 H, NH), 12.34–12.95 (br s, 1 H, COOH); ^{13}C NMR (DMSO-d_6) δ 171.14, 168.90, 166.32, 134.25, 129.42, 126.56, 125.67, 123.43, 63.35, 22.93. Anal. ($C_{11}H_{12}N_2O_5$) C, H, N.

110: mp 215–217 °C (ethanol); IR (mineral oil) 3400–2700, 1700, 1650 cm^{-1}; MS *m/z* 282 (M^+); ^{1}H NMR (300 MHz, DMSO-d_6) δ 2.09 (s, 3 H, $NCOCH_3$), 3.64 (br s, 2 H, OH), 4.05–4.15 (m, 1 H, CH_2OH), 4.88–4.94 (m, 1 H, CH_2OH), 5.77–5.85 (m, 1 H, CHOH), 7.56–7.78 (m, 2 H, aromatic), 8.20–8.29 (m, 1 H, aromatic), 9.40 (br s, 1 H, NH), 9.63 (br s, 1 H, NH), 12.81 (br s, 1 H, COOH); ^{13}C NMR (DMSO-d_6) δ 171.45, 168.60, 166.24, 134.20, 129.42, 126.56, 123.43, 72.76, 63.35, 22.99. Anal. ($C_{12}H_{14}N_2O_6$) C, H, N.

4-(Acetylamino)-3-[(aminoacetyl)amino]benzoic Acid, Hydrochloride (111) and 4-(Acetylamino)-3-[(4-aminobutanoyl)amino]benzoic Acid, Hydrochloride (112). Compound **7** (80 mg, 0.24 mmol) or **8** (60 mg, 0.17 mmol) was added to cold 0.1 N NaOH (2 mL for **7**, 1.5 mL for **8**), and the mixture was stirred at 0 °C for 1 h. The solution was adjusted to pH 7 by the addition of 5% HCl (1.5 mL) and concentrated to dryness on a rotary evaporator. The residue obtained was dissolved in water, the insoluble material filtered, and the filtrate adjusted to pH 2–3 by the addition of 5% HCl (2–4 mL). The acidic solution was then concentrated to one-third its volume, and the separated solid was filtered and dried to give **111** (60 mg, 84% yield) or **112** (43 mg, 81% yield) as white solids.

111: mp 220–223 °C dec (ethanol/ether); IR (mineral oil) 2700–3400, 1700, 1650 cm^{-1}; ^{1}H NMR (300 MHz, DMSO-d_6) δ 2.16 (s, 3 H, $NCOCH_3$), 3.85–3.96 (s, 2 H, CH_2N), 7.69–7.77 (m, 1 H, aromatic), 7.93–8.00 (m, 1 H, aromatic), 8.14–8.21 (m, 1 H, aromatic), 8.26–8.37 (br s, 3 H, NH_3^+), 9.90–10.05 (br s, 1 H, NH), 10.50–10.65 (br s, 1 H, NH). Anal. ($C_{11}H_{13}N_3O_4$·HCl) C, H, N, Cl.

112: mp 236–240 °C dec (ethanol/ether); IR (mineral oil) 3400–2700, 1690, 1650 cm^{-1}; ^{1}H NMR (300 MHz, D_2O) δ 1.89–1.92 (s, $CH_3CO_2^-$), 1.98–2.10 (m, 2 H, $CH_2CH_2CH_2$), 2.16–2.20 (s, 3 H, $NCOCH_3$), 2.55–2.64 (m, 2 H, $COCH_2$), 3.05–3.13 (m, 2 H, NCH_2), 7.46–7.52 (m, 1 H, aromatic), 7.76–7.83 (m, 1 H, aromatic), 7.83–7.88 (m, 1 H, aromatic). Anal. ($C_{13}H_{16}N_3O_4$·HCl) C, H, N, Cl.

4-(Acetylamino)-3-guanidinobenzoic Acid, Hydrochloride (113). To compound **108** (0.500 g, 2.57 mmol) were added concentrated HCl (0.25 mL), H_2O (0.25 mL), and cyanamide (0.350 g, 8.33 mmol). The mixture was heated at 60–80 °C with stirring for 15–20 min until the solid mass became a clear melt. The mixture was cooled in an ice bath, diluted with water (7–8 mL), acidified with concentrated HCl (2.5 mL), and cooled at −5 °C. After 2–3 h the solid crystallized, was filtered, and was washed on the filter with ice cold 5% HCl to give **13** (0.408 g, 68.8% yield) as a white solid: mp 203–205 °C (ethanol/ether); IR (mineral oil) 3500–3100, 1700–1630, 1590, 1520, 1300 cm^{-1}; ^{1}H NMR (300 MHz, DMSO-d_6) δ 2.14 (s, 3 H, $NCOCH_3$), 7.50 (br s, 4 H, NH_2), 7.75 (m, 1 H, ArH), 7.89 (m, 2 H, ArH), 9.1 (s, 1 H, NH), 10.01 (s, 1 H, NH); ^{13}C NMR (DMSO-d_6) δ 171.59, 168.69, 159.04, 140.67, 131.05, 130.90, 129.49, 128.69, 125.70, 26.17. Anal. ($C_{10}H_{13}N_4O_3Cl$) C, H, N, Cl.

Inhibition Assay. All compounds were evaluated for *in vitro* inhibitory actions on influenza N2 (A/Tokyo/67) and influenza type B (B/Memphis/3/89) sialidases in whole virus. The details of these procedures have been published.[23] Briefly, for each virus type the sialidase gene was reassorted into a high-growth genetic background. The inhibition assays were then performed using two methods. One assay employed monitoring the fluorescence of 4-methylumbelliferone released from the small substrate (4-methylumbelliferyl)-*N*-acetylneuraminic acid (MUN). The second utilized the high molecular weight substrate fetuin and detected released sialic acid by the standard thiobarbituric acid colorimetric assay. The IC_{50} values were determined graphically and are summarized in Table 2.

Crystallization and Inhibitor Soaking. Native crystals of A/Tokyo/3/67 were grown by the hanging drop method using purified sialidase heads. The space group of our N2 crystals is orthorhombic $C222_1$[17] with a = 119.70, b = 138.29, and c = 139.98 Å. The N2–inhibitor complexes were prepared by soaking the native N2 crystals in the soaking buffer containing 5 mM inhibitors for about 8 h. The soaking buffer contained 0.10 M sodium phosphate, 0.15 M sodium chloride, 5% DMSO, and 12.5% PEG 4000 at pH 6.3. The B/Lee/40 native crystals were grown as previously described[24] (space group $P42_12$, a = 125.4 and c = 72.2 Å), and the inhibitor at 5 mM concentration was soaked into the crystal in a solution of 15% PEG 3350, 2 M sodium nitrate, 0.15 M sodium chloride, and 2 mM calcium chloride. The diffraction data were collected at room temperature on a SIEMENS multiwire area detector mounted an a RIGAKU rotating anode X-ray generator RU-200 using Cu Kα radiation. The data were processed using the XENGEN package. The inhibitor was included by building the molecule into $||F_o| - |F_c||$ electron density maps using an Evans and Southerland PS-300 graphics system with FRODO software,[19] after initial rigid body refinements of the protein component using X-plor.[28] Water molecules and sugar chains were later fitted in the $||F_o| - |F_c||$ electron density maps calculated after refinement of the sialidase–inhibitor complexes by X-plor. Finally, conjugate gradient and molecular dynamics refinements were then performed using X-plor and data between 6.5 Å and the highest resolution of the data (1.8 or 2.4 Å). The final maps were determined using the calculated phases from

refined coordinates without the inclusion of inhibitor. The electron density maps in Figures 1–3 were contoured at 1σ.

Acknowledgment. We thank Aleta Dean and Dr. Gary G. Hu for excellent technical assistance. This work was supported by NIH grants to M.L. (U01 Al31888) and G.M.A. (R01 Al26718).

References

(1) Air, G. M.; Laver, W. G. The Neuraminidase of Influenza Virus. *Proteins: Struct., Funct., Genet.* **1989**, *6*, 341–356.

(2) (a) Holzer, C. T.; von Itzstein, M.; Jin, B.; Pegg, M. S.; Stewart, W. P.; Wu, W.-Y. Inhibition of Sialidases from Viral, Bacterial and Mammalian Sources by Analogues of 2-Deoxy-2,3-didehydro-*N*-acetylneuraminic Acid Modified at the C-4 Position. *Glycoconj. J.* **1993**, *10*, 40–44. (b) Ryan, D. M.; Ticehurst, J.; Dempsey, M. H.; Penn, C. R. Inhibition of Influenza Virus Replication in Mice by GG167 (4-Guanidino-2,4-dideoxy-2,3-dehydro-*N*-acetylneuraminic Acid) is Consistent with Extracellular Activity of Viral Neuraminidase (Sialidase). *Antimicrob. Agents Chemother.* **1994**, *38*, 2270–2275.

(3) (a) Meindl, P.; Tuppy, H. 2-Deoxy-2,3-dehydrosialic Acids. I. Synthesis and Properties of 2-Deoxy-2,3-dehydro-*N*-acetylneuraminic Acids and their Methyl Esters. *Monatsh. Chem.* **1969**, *100*, 1295–1306. (b) Meindl, P.; Bodo, G.; Lindner, J.; Palese, P. Influence of 2-Deoxy-2,3-dehydro-*N*-acetylneuraminic Acid on Myxovirus Neuraminidases and the Replication of Influenza and Newcastle Disease Virus. *Z. Naturforsch.* **1971**, *263*, 792–797. (c) Meindl, P.; Bodo, G.; Palese, P.; Schulman, J.; Tuppy, H. Inhibition of Neuraminidase Activity by Derivatives of 2-Deoxy-2,3-dehydro-*N*-acetylneuraminic Acid. *Virology* **1974**, *58*, 457–463.

(4) Burmeister, W. P.; Ruigrok, R. W. H.; Cusack, S. The 2.2Å Resolution Crystal Structure of Influenza B Neuraminidase and its Complex with Sialic Acid. *EMBO J.* **1992**, *11*, 49–56.

(5) Baker, A. T.; Varghese, J. N.; Laver, W. G.; Air, G. M.; Colman, P. M. Three-dimensional Structure of Neuraminidase of Subtype N9 from an Avian Influenza Virus. *Proteins: Struct., Funct., Genet.* **1987**, *2*, 111–117.

(6) Janakiraman, M. N.; White, C. L.; Laver, W. G.; Air, G. M.; Luo, M. Structure of Influenza Virus Neuraminidase B/Lee/40 Complexed with Sialic Acid and a Dehydro Analog at 1.8Å Resolution: Implication for the Catalytic Mechanism. *Biochemistry* **1994**, *33*, 8172–8179.

(7) Tulip, W. R.; Varghese, J. N.; Baker, A. T.; van Donkelaar, A.; Laver, W. G.; Webster, R. G.; Colman, P. M. Refined Atomic Structures of N9 Subtype Influenza Virus Neuraminidase and Escape Mutants. *J. Mol. Biol.* **1991**, *221*, 487–497.

(8) Varghese, J. N.; McKimm-Breschkin, J. L.; Caldwell, J. B.; Kortt, A. A.; Colman, P. M. The Structure of the Complex Between Influenza Virus Neuraminidase and Sialic Acid, the Viral Receptor. *Proteins* **1992**, *14*, 327–332.

(9) Bossart-Whitaker, P.; Carson, M.; Babu, Y. S.; Smith, C. D.; Laver, W. G.; Air, G. M. Three-dimensional Structure of Influenza A N9 Neuraminidase and its Complex with the Inhibitor 2-Deoxy-2,3-Dehydro-*N*-Acetyl Neuraminic Acid. *J. Mol. Biol.* **1993**, *232*, 1069–1083.

(10) Varghese, J. N.; Colman, P. M. Three-dimensional Structure of the Neuraminidase of Influenza Virus A/Tokyo/3/67 at 2.2Å Resolution. *J. Mol. Biol.* **1991**, *221*, 473–486.

(11) Varghese, J. N.; Laver, W. G.; Colman, P. M. Structure of the Influenza Virus Glycoprotein Antigen Neuraminidase at 2.9Å Resolution. *Nature (London)* **1983**, *303*, 35–40.

(12) von Itzstein, M.; Wu, W.-Y.; Kok, G. B.; Pegg, M. S.; Dyason, J. C.; Jin, B.; Phan, T. V.; Smythe, M. L.; White, H. F.; Oliver, S. W.; Colman, P. M.; Varghese, J. N.; Ryan, D. M.; Woods, J. M.; Bethell, R. C.; Hotham, V. J.; Cameron, J. M.; Penn, C. R. Rational Design of Potent Sialidase-Based Inhibitors of Influenza Virus Replication. *Nature* **1993**, *363*, 418–423.

(13) von Itzstein, M.; Wu, W.-Y.; Jin, B. The Synthesis of 2,3-Didehydro-2,4-dideoxy-4-guanidyl-*N*-acetylneuraminic Acid: A Potent Influenza Sialidase Inhibitor. *Carbohydr. Res.* **1994**, *259*, 301–305.

(14) Pegg, M. S.; von Itzstein, M. Slow-binding Inhibition of Sialidase from Influenza Virus. *Biochem. Mol. Biol. Int.* **1994**, *32*, 851–858.

(15) Nöhle, U.; Beau, J.-M.; Schauer, R. Uptake, Metabolism and Excretion of Orally and Intravenously Administered, Double-Labeled *N*-Glycolylneuraminic Acid and Single-Labeled 2-Deoxy-2,3-dehydro-*N*-acetylneuraminic Acid in Mouse and Rat. *Eur. J. Biochem.* **1982**, *126*, 543–548.

(16) Thomas, G. P.; Forsyth, M.; Penn, C. R.; McCauley, J. W. Inhibition of the Growth of Influenza Viruses in vitro by 4-Guanidino-2,4-dideoxy-*N*-acetylneuraminic Acid. *Antiviral Res.* **1994**, *24*, 351–356.

(17) Jedrzejas, M. J.; Singh, S.; Brouillette, W. J.; Laver, W. G.; Air, G. M.; Luo, M. Structures of Aromatic Inhibitors of Influenza Virus Neuraminidase. *Biochemistry* **1995**, *34*, 3144–3151.

(18) Meindl, P.; Bodo, G.; Lindner, J.; Palese, P. Influence of 2-Deoxy-2,3-dehydro-*N*-acetylneuraminic Acid on Myxovirus Neuraminidases and the Replication of Influenza and Newcastle Disease Virus. *Z. Naturforsch.* **1971**, *263*, 792–797.

(19) Jones, T. A. Diffraction Methods for Biological Macromolecules. Interactive Computer Graphics: FRODO. *Methods Enzymol.* **1985**, *115*, 157–171.

(20) Jedrzejas, M. S.; Singh, S.; Air, G. M.; Brouillette, W. J.; Luo, M. Unpublished results.

(21) Gilson, M. K.; Sharp, K. A.; Honig, B. H. Calculating the Electrostatic Potential of Molecules in Solution. *J. Comput. Chem.* **1988**, *9*, 327–335.

(22) Goodford, P. J. A. Computational Procedure for Determining Energetically Favorable Binding Sites on Biologically Important Macromolecules. *J. Med. Chem.* **1985**, *28*, 849–857.

(23) Aymard-Henry, M.; Coleman, M. T.; Dowdie, W. R.; Laver, W. G.; Shild, G. C.; Webster, R. G. Influenza Virus Neuraminidase and Neuraminidase Inhibition Test Procedures. *Bull. W. H. O.* **1973**, *48*, 199–202.

(24) Lin, Y. New Crystalline Forms of Neuraminidase of Type B Human Influenza Virus. *J. Mol. Biol.* **1990**, *214*, 639–640.

(25) Taylor, N. R.; von Itzstein, M. Molecular Modeling Studies on Ligand Binding to Sialidase from Influenza Virus and the Mechanism of Catalysis. *J. Med. Chem.* **1994**, *37*, 616–624.

(26) Kasuya, F.; Igarashi, K.; Fukui, M. Metabolism of Benoxinate in Humans. *J. Pharm. Sci.* **1987**, *76*, 303–305.

(27) Appleton, J. M.; Andrews, B. D.; Rae, I. D.; Reichert, B. E. Aromatic Amides. Intermolecular Hydrogen Bonding in Ortho-substituted Anilides. *Aust. J. Chem.* **1970**, *23*, 1667–1677.

(28) Brunger, A. T. *X-PLOR Version 3.1: A System for X-ray Crystallography and NMR*; Yale University Press: New Haven, CT, 1992; pp 1–382.

JM940788U